Electronic Supplementary Information: Optimizing External Quantum Efficiency in Photocatalysts via First-Principles Optics and Carrier Transport Modeling

Masanori Kaneko

Graduate School of Nanobioscience, Yokohama City University 22-2 Seto, Kanazawa-ku, Yokohama 236-0027 Japan

Hiroaki Yoshida

Science and Innovation Center, Mitsubishi Chemical Corporation, Aoba-ku, Yokohama-shi, Kanagawa, Japan and Japan Technological Research Association of Artificial Photosynthetic Chemical Process (ARPChem), Tokyo, Japan

Koichi Yamashita

Graduate School of Nanobioscience, Yokohama City University 22-2 Seto, Kanazawa-ku, Yokohama 236-0027 Japan

Kazunari Domen

Research Initiative for Supra-Materials, Interdisciplinary Cluster for Cutting Edge Research, Shinshu University, Nagano, Japan and Office of University Professors, The University of Tokyo, Bunkyo-ku, Tokyo, Japan

Kazuhiko Seki*

Global Zero Emission Research Center, National Institute of Advanced Industrial Science and Technology (AIST), Tsukuba 16-1 Onogawa, Tsukuba, Ibaraki 305-8569 Japan

I. DERIVATION OF EQN (6) AND (7)

We follow the formulation of Sec. 86, Problem 4 in Ref. 1, which considers a plane-parallel layer (region 2) situated between vacuum (region 1) and another medium (region 3). By invoking the principle of optical reversibility among the incident, reflected, and transmitted waves, the reflection amplitude is given by

$$r_{\mathrm{A}} = \frac{r_{12} + r_{23}\exp(2i\psi)}{1 + r_{12}r_{23}\exp(2i\psi)}, \tag{S1}$$

where $\psi = \omega L\sqrt{\epsilon_2 - \epsilon_1 \sin^2\theta_0}/c$ denotes the phase accumulation across a layer of thickness L, ω is the angular frequency, c is the speed of light, ϵ_2 is the permittivity of region 2, and θ_0 is the angle of incidence with respect to the surface normal.

The interface reflection coefficient r_{ij}, defined as the amplitude ratio of the reflected to incident field at the boundary between media i and j in the limit $L \to \infty$, is given by[1]

$$r_{ij} = \frac{\sqrt{\epsilon_i}\cos\theta_i - \sqrt{\epsilon_j}\cos\theta_j}{\sqrt{\epsilon_i}\cos\theta_i + \sqrt{\epsilon_j}\cos\theta_j}, \tag{S2}$$

where Snell's law relates the angles via $\sqrt{\epsilon_i}\sin\theta_i = \sqrt{\epsilon_j}\sin\theta_j$. Substituting this into eqn (S2) yields

$$r_{ij} = \frac{\sqrt{\epsilon_i}\cos\theta_i - \sqrt{\epsilon_j - \epsilon_i\sin^2\theta_i}}{\sqrt{\epsilon_i}\cos\theta_i + \sqrt{\epsilon_j - \epsilon_i\sin^2\theta_i}}. \tag{S3}$$

In the limit $L \to 0$, eqn (S1) reduces to

$$r_{13} = \frac{r_{12} + r_{23}}{1 + r_{12}r_{23}}, \tag{S4}$$

which can be rearranged as

$$r_{23} = \frac{r_{12} - r_{13}}{r_{12}r_{13} - 1}. \tag{S5}$$

If both media 1 and 3 are vacuum ($r_{13} = 0$), then $r_{23} = -r_{12}$.

The reflectance is calculated as

$$r_{\mathrm{fl}} = |r_{\mathrm{A}}|^2 = \frac{|r_{12}|^2 + |r_{23}|^2\exp[2i(\psi - \psi^*)] + r_{12}r_{23}^*\exp(-2i\psi^*) + r_{12}^*r_{23}\exp(2i\psi)}{1 + |r_{12}|^2|r_{23}|^2\exp[2i(\psi - \psi^*)] + r_{12}r_{23}\exp(2i\psi) + r_{12}^*r_{23}^*\exp(-2i\psi^*)}. \tag{S6}$$

The transmission amplitude is given by[1]

$$t_{\mathrm{A}} = \frac{(1 - r_{12}^2)\exp(i\psi)}{1 + r_{12}r_{23}\exp(2i\psi)}, \tag{S7}$$

with the corresponding transmittance:

$$t_{\mathrm{rans}} = |t_{\mathrm{A}}|^2 = \frac{(1 - |r_{12}|)^2\exp[i(\psi - \psi^*)]}{1 + |r_{12}|^2|r_{23}|^2\exp[2i(\psi - \psi^*)] + r_{12}r_{23}\exp(2i\psi) + r_{12}^*r_{23}^*\exp(-2i\psi^*)}. \tag{S8}$$

For normal incidence ($\theta_0 = 0$) and vacuum in region 1 ($n_1 = 1$), the phase is

$$\psi = \omega L\sqrt{\epsilon_2}\,/c = \omega L(n_2 + i\kappa_2)/c, \tag{S9}$$

and we find,

$$\exp(2i\psi) = \exp(2\omega L(in_2 - \kappa_2)/c), \tag{S10}$$

where n_2 and κ_2 are the real and imaginary parts of the complex refractive index of region 2.

When media 1 and 3 are both vacuum ($r_{13} = 0$), then $r_{23} = -r_{12}$ and the reflectance becomes

$$r_{\mathrm{fl}} = \frac{|r_{12}|^2\left[1 + e^{-2\alpha L} - 2\cos(2\omega Ln_2/c)e^{-\alpha L}\right]}{1 + |r_{12}|^4e^{-2\alpha L} - 2\left[\mathrm{Re}(r_{12}^2)\cos(2\omega Ln_2/c) - \mathrm{Im}(r_{12}^2)\sin(2\omega Ln_2/c)\right]e^{-\alpha L}}, \tag{S11}$$

with $\alpha = 2\omega\kappa_2/c$. The transmittance is given by

$$t_{\mathrm{rans}} = \frac{(1 - |r_{12}|)^2e^{-\alpha L}}{1 + |r_{12}|^4e^{-2\alpha L} - 2\left[\mathrm{Re}(r_{12}^2)\cos(2\omega Ln_2/c) - \mathrm{Im}(r_{12}^2)\sin(2\omega Ln_2/c)\right]e^{-\alpha L}}. \tag{S12}$$

To account for random initial phase δ, we let $\psi = \omega L\sqrt{\epsilon_2}/c + \delta$, resulting in $\cos(2\omega Ln_2/c + 2\delta)$ and $\sin(2\omega Ln_2/c + 2\delta)$ terms. In principle, averaging should be performed after computing the effective reflectivity R_{eff}, but for simplicity, we perform a pre-averaging over δ using $\int_0^{2\pi} d\delta\cos(2\omega Ln_2/c + 2\delta)/(2\pi) = 0$, $\int_0^{2\pi} d\delta\sin(2\omega Ln_2/c + 2\delta)/(2\pi) = 0$ and similar terms. By expanding in series and using trigonometric identities, we obtain the phase-averaged reflectance:[2]

$$r_{\mathrm{fl}} \approx \frac{|r_{12}|^2\left[1 + (1 - 2\left[(\mathrm{Re}\,r_{12})^2 - (\mathrm{Im}\,r_{12})^2\right])\exp\left(-2\alpha L\right)\right]}{1 - |r_{12}|^4\exp\left(-2\alpha L\right)}, \tag{S13}$$

where $\mathrm{Re}\,r_{12}$ and $\mathrm{Im}\,r_{12}$ denote the real and imaginary parts of r_{12}. In deriving eqn (S13), we used the identities $\mathrm{Re}(r_{12}^2) = (\mathrm{Re}\,r_{12})^2 - (\mathrm{Im}\,r_{12})^2$ and $\mathrm{Im}(r_{12}^2) = 2\,\mathrm{Re}(r_{12})\,\mathrm{Im}(r_{12})$. For normal incidence ($\mathrm{Im}(r_{12}) = 0$), eqn (S13) reduces to

$$r_{\mathrm{fl}} = |r_{12}|^2 + \frac{|r_{12}|^2(1 - |r_{12}|^2)^2\exp\left(-2\alpha L\right)}{1 - |r_{12}|^4\exp\left(-2\alpha L\right)}. \tag{S14}$$

This expression corresponds to eqn (7). Similarly, the transmittance becomes

$$t_{\mathrm{rans}} \approx \frac{(1-|r_{12}|)^2 \exp(-\alpha L)}{1-|r_{12}|^4 \exp(-2\alpha L)}, \tag{S15}$$

which corresponds to eqn (6). Eqn (S13) and (S15) can also be derived from eqn (S11) and (S12), respectively, without resorting to a series expansion, by applying the following integral identities,[3–6]

$$\frac{1}{2\pi}\int_0^{2\pi} d\theta \frac{\cos(x+2\theta)}{1+C_1^2+C_2^2-2C_1\cos(x+2\theta)+2C_2\sin(x+2\theta)} = \frac{C_1}{1-C_1^2-C_2^2}, \tag{S16}$$

$$\frac{1}{2\pi}\int_0^{2\pi} d\theta \frac{1}{1+C_1^2+C_2^2-2C_1\cos(x+2\theta)+2C_2\sin(x+2\theta)} = \frac{1}{1-C_1^2-C_2^2}, \tag{S17}$$

which are valid under the conditions $1 > C_1^2 + C_2^2$ and $(C_1^2 + C_2)^{1/4} < 1$. The latter condition ensures that $|r_{12}| < 1$.

II. TRANSFER MATRIX DERIVED FROM SCATTERING MATRIX

For convenience, we rewrite eqn (5) in the form used in the transfer matrix method,

$$\begin{pmatrix} I_A \\ j_A \end{pmatrix} = \begin{pmatrix} T_{11} & T_{12} \\ T_{21} & T_{22} \end{pmatrix} \begin{pmatrix} I_1 \\ j_1 \end{pmatrix}, \tag{S18}$$

where the elements are given by,

$$T_{11} = t_{11} - \frac{t_{12}t_{21}}{t_{22}} = (1-R)\exp(-\alpha L), \tag{S19}$$

$$T_{12} = \frac{t_{12}}{t_{22}} = R\exp(-\alpha L), \tag{S20}$$

$$T_{21} = -T_{12} = -R\exp(-\alpha L), \tag{S21}$$

$$T_{22} = \frac{1}{t_{22}} = \frac{1-R^2\exp(-2\alpha L)}{(1-R)\exp(-\alpha L)}. \tag{S22}$$

For the second layer from the top, let I_2 denote the portion of incident photon flux that enters from above without being reflected at the interface, and let j_2 denote the flux transmitted upward from the layer, originating from incident light that has entered the layer from both sides. Neglecting light absorption by air, we have,

$$\begin{pmatrix} I_2 \\ j_2 \end{pmatrix} = \begin{pmatrix} 1-R & R \\ -R & 1+R \end{pmatrix} \begin{pmatrix} I_A \\ j_A \end{pmatrix}. \tag{S23}$$

By eliminating I_A and j_A using eqn (S18) and (S23), we obtain,

$$\begin{pmatrix} I_2 \\ j_2 \end{pmatrix} = \begin{pmatrix} 1-R & R \\ -R & 1+R \end{pmatrix} \begin{pmatrix} (1-R)\exp(-\alpha L) & R\exp(-\alpha L) \\ -R\exp(-\alpha L) & \dfrac{1-R^2\exp(-2\alpha L)}{(1-R)\exp(-\alpha L)} \end{pmatrix} \begin{pmatrix} I_1 \\ j_1 \end{pmatrix}. \tag{S24}$$

We define the transfer matrix T_{d} (for downward transfer) from eqn (S24) and obtain,

$$\begin{pmatrix} I_m \\ j_m \end{pmatrix} = T_{\mathrm{d}}^{m-1} \begin{pmatrix} I_1 \\ j_1 \end{pmatrix}, \tag{S25}$$

where T_{d} is given by,

$$T_{\mathrm{d}} = \begin{pmatrix} 1-R & R \\ -R & 1+R \end{pmatrix} \begin{pmatrix} (1-R)\exp(-\alpha L) & R\exp(-\alpha L) \\ -R\exp(-\alpha L) & \dfrac{1-R^2\exp(-2\alpha L)}{(1-R)\exp(-\alpha L)} \end{pmatrix} \tag{S26}$$

$$= \begin{pmatrix} (1-2R)\exp(-\alpha L) & R\dfrac{1+(1-2R)\exp(-2\alpha L)}{(1-R)\exp(-\alpha L)} \\ -2R\exp(-\alpha L) & \dfrac{1+R-2R^2\exp(-2\alpha L)}{(1-R)\exp(-\alpha L)} \end{pmatrix}. \tag{S27}$$

Let λ_1 and λ_2 be the eigenvalues of T_{d}, with $\lambda_1 > \lambda_2$. Then,

$$\mathrm{Tr}(T_{\mathrm{d}}) = \lambda_1 + \lambda_2 = 2\cosh(\alpha L) + \frac{4R\sinh(\alpha L)}{1-R} > 0,$$

and $\det(T_{\mathrm{d}}) = \lambda_1\lambda_2 = 1$. We define the characteristic polynomial of the 2×2 matrix T_{d} as $f(\lambda) = (\lambda - \lambda_1)(\lambda - \lambda_2)$. Note that $f(0) = \det(T_{\mathrm{d}}) = 1 > 0$, and the minimum of $f(\lambda)$ occurs at $\mathrm{Tr}(T_{\mathrm{d}})/2 > 0$. Since $f(1) = 1 - (\lambda_1 + \lambda_2) + \lambda_1\lambda_2 = 2 - \lambda_1 - \lambda_2 < 0$, it follows that $\lambda_1 > 1 > \lambda_2 > 0$. The discriminant of the characteristic polynomial confirms that the eigenvalues are real and distinct, $\lambda_1 - \lambda_2 = \sqrt{(\lambda_1 + \lambda_2)^2 - 4\lambda_1\lambda_2} > 0$.

III. EXACT SOLUTION FOR AN INFINITE STACK OF LAYERS

By noticing that K, the fraction of light absorbed by a single layer with absorption coefficient α and thickness L, is identical for each layer, and that the total photon flux entering each layer from above and below, without being reflected at the interfaces, is given by $\sum_{m=1}^{\infty}(I_m + j_{m+1})$, the EQE under the assumption of an IQE equal to unity is expressed as,

$$\mathrm{A_{bs}} = K\sum_{m=1}^{\infty}\left(I_m + j_{m+1}\right)/I_0 \tag{S28}$$

$$= K(1-R)\sum_{m=1}^{\infty}\left(I_m + j_{m+1}\right)/I_1, \tag{S29}$$

where $I_1 = (1-R)I_0$, and the transmitted light, scaled by the factor $(1-R)$, is assumed to be absorbed by the particle layers.

Using eqn (9) and eqn (10), each component can be expressed as,

$$I_m = \frac{\lambda_1^{m-1} - \lambda_2^{m-1}}{\lambda_1 - \lambda_2}\left[(T_\mathrm{d})_{11}I_1 + (T_\mathrm{d})_{12}j_1\right] - \frac{\lambda_1^{m-2} - \lambda_2^{m-2}}{\lambda_1 - \lambda_2}\lambda_1\lambda_2 I_1, \tag{S30}$$

$$j_m = \frac{\lambda_1^{m-1} - \lambda_2^{m-1}}{\lambda_1 - \lambda_2}\left[(T_\mathrm{d})_{21}I_1 + (T_\mathrm{d})_{22}j_1\right] - \frac{\lambda_1^{m-2} - \lambda_2^{m-2}}{\lambda_1 - \lambda_2}\lambda_1\lambda_2 j_1. \tag{S31}$$

Summing over m yields,

$$\begin{aligned}\sum_{m=1}^{N} I_m = {} & \frac{\left(1-\lambda_1^N\right)\left[\left((T_\mathrm{d})_{11} - \lambda_2\right)I_1 + (T_\mathrm{d})_{12}j_1\right]}{(1-\lambda_1)(\lambda_1-\lambda_2)} \\ & - \frac{\left(1-\lambda_2^N\right)\left[\left((T_\mathrm{d})_{11} - \lambda_1\right)I_1 + (T_\mathrm{d})_{12}j_1\right]}{(1-\lambda_2)(\lambda_1-\lambda_2)},\end{aligned} \tag{S32}$$

$$\begin{aligned}\sum_{m=2}^{N} j_m = {} & \frac{\left(\lambda_1-\lambda_1^{N+1}\right)\left[(T_\mathrm{d})_{21}I_1 + \left((T_\mathrm{d})_{22} - \lambda_2\right)j_1\right]}{(1-\lambda_1)(\lambda_1-\lambda_2)} \\ & - \frac{\left(\lambda_2-\lambda_2^{N+1}\right)\left[(T_\mathrm{d})_{21}I_1 + \left((T_\mathrm{d})_{22} - \lambda_1\right)j_1\right]}{(1-\lambda_2)(\lambda_1-\lambda_2)}.\end{aligned} \tag{S33}$$

Using the relation $R_\mathrm{eff} = R + j_1/I_0$ and $\mathrm{A_{bs}} = 1 - R_\mathrm{eff}$, we obtain

$$j_1 = \frac{R_\mathrm{eff} - R}{1-R}I_1 = \frac{1 - \mathrm{A_{bs}} - R}{1-R}I_1. \tag{S34}$$

For sufficiently large value N, and given that $\lambda_1 > 1 > \lambda_2 > 0$, eqn (S32) and (S33) can be approximated as

$$\sum_{m=1}^{N} I_m \approx \left(-\lambda_1^N\right) \frac{\left[(T_\mathrm{d})_{11} - \lambda_2\right] I_1 + (T_\mathrm{d})_{12}\, j_1}{(1-\lambda_1)(\lambda_1 - \lambda_2)}, \tag{S35}$$

$$\sum_{m=2}^{N} j_m \approx \left(-\lambda_1^N\right) \frac{(T_\mathrm{d})_{21}\, I_1 + \left[(T_\mathrm{d})_{22} - \lambda_2\right] j_1}{(1-\lambda_1)(\lambda_1 - \lambda_2)}. \tag{S36}$$

Substituting eqn (S35) and (S36) into eqn (S29), and eliminating j_1 using eqn (S34), yields a closed-form expression for $\mathrm{A_{bs}}$,

$$\frac{\mathrm{A_{bs}}}{K(1-R)} \approx \sum_{m=1}^{N} \left(I_m + j_{m+1}\right)/I_1 \tag{S37}$$

$$\approx \left(-\lambda_1^N\right) \left[\frac{(T_\mathrm{d})_{11} + (T_\mathrm{d})_{21} - \lambda_2}{(1-\lambda_1)(\lambda_1-\lambda_2)} + \frac{(T_\mathrm{d})_{12} + (T_\mathrm{d})_{22} - \lambda_2}{(1-\lambda_1)(\lambda_1-\lambda_2)} \cdot \frac{1 - \mathrm{A_{bs}} - R}{1-R}\right]. \tag{S38}$$

Rearranging eqn (S38) leads to

$$\frac{\mathrm{A_{bs}}}{1-R}\left(\frac{1}{K} + \left(-\lambda_1^N\right)\frac{(T_\mathrm{d})_{12} + (T_\mathrm{d})_{22} - \lambda_2}{(1-\lambda_1)(\lambda_1-\lambda_2)}\right) = \left(-\lambda_1^N\right)\frac{(T_\mathrm{d})_{11} + (T_\mathrm{d})_{21} + (T_\mathrm{d})_{12} + (T_\mathrm{d})_{22} - 2\lambda_2}{(1-\lambda_1)(\lambda_1-\lambda_2)}. \tag{S39}$$

Taking the limit $N \to \infty$, we finally obtain

$$\mathrm{A_{bs}} = (1-R)\frac{(T_\mathrm{d})_{11} + (T_\mathrm{d})_{21} + (T_\mathrm{d})_{12} + (T_\mathrm{d})_{22} - 2\lambda_2}{(T_\mathrm{d})_{12} + (T_\mathrm{d})_{22} - \lambda_2}, \tag{S40}$$

$$= (1-R)\left[1 + \frac{(T_\mathrm{d})_{11} + (T_\mathrm{d})_{21} - \lambda_2}{(T_\mathrm{d})_{12} + (T_\mathrm{d})_{22} - \lambda_2}\right]. \tag{S41}$$

Eqn (S41) can be considered exact, since the approximations made in eqn (S35) and (S36) are fully justified in the limit $N \to \infty$. Here, we considered an infinite stack of layers, thereby avoiding the need to impose a boundary condition at the bottom layer when the incident light enters from the top. Eqn (16) and (S41) yield the characteristic polynomial $\lambda_2^2 - \mathrm{Tr}(T_\mathrm{d})\lambda_2 + \det(T_\mathrm{d}) = 0$, which follows from the fact that λ_2 is one of the eigenvalues of the 2×2 matrix T_d. Therefore, these equations are found to be exactly equivalent.

IV. ESTIMATION OF SOLAR-TO-HYDROGEN (STH) CONVERSION EFFICIENCY

The solar-to-hydrogen (STH) conversion efficiency is calculated by integrating the product of the quantum efficiency (or quantum yield), $Y(\lambda)$, and the spectral photon flux of the incident solar spectrum over the relevant wavelength range. It is expressed as

$$\mathrm{STH}(\%) = \frac{1.23\ \mathrm{eV}}{P_{\mathrm{in}}} \int d\lambda\, Y(\lambda)\, \Phi(\lambda) \times 100, \tag{S42}$$

where $\Phi(\lambda)$ is the spectral photon flux (in units of photons $\mathrm{cm}^{-2}\,\mathrm{s}^{-1}\,\mathrm{nm}^{-1}$), λ is the wavelength in nanometers, and 1.23 eV corresponds to the Gibbs free energy required to drive overall water splitting under standard conditions. The incident power density, P_{in}, is taken as the total integrated irradiance of the Air Mass 1.5 Global (AM 1.5G) solar spectrum, approximately 100 $\mathrm{mW\,cm^{-2}}$ (equivalent to 1.0 $\mathrm{kW\,m^{-2}}$).[7] Eqn (S42) assumes 100% Faradaic efficiency and neglects kinetic, catalytic, and overpotential losses.

When considering only IQE, under the assumption that all absorbed photons generate charge carriers, $Y(\lambda)$ is given by $I_{qe}(\lambda)$. When carrier generation follows a depth-dependent profile governed by the Lambert–Beer law, $Y(\lambda) = I_{qe}(\lambda)$ is evaluated using eqn (S46), incorporating the wavelength-dependent absorption coefficient $\alpha(\lambda)$ obtained via DFT/HSE06 calculations.[8] For the special case of uniform carrier generation, $Y(\lambda)$ is approximated by a constant value I_{qe0}, derived from eqn (33). These calculations enable quantitative comparisons of STH efficiency under different spatial profiles of carrier generation.

To account for optical losses due to incomplete absorption, $Y(\lambda)$ is expressed as the product $I_{qe}(\lambda)\, A_{\mathrm{bs}}(\lambda)$, where $A_{\mathrm{bs}}(\lambda)$ denotes the spectral absorptance of the photocatalyst. In this framework, $I_{qe}(\lambda)$ may be approximated by I_{qe0}, while $A_{\mathrm{bs}}(\lambda)$ may be replaced by either $A_{\mathrm{bss}}(\lambda)$ or $A_{\mathrm{bsem}}(\lambda)$, depending on the optical model adopted.

The solar-to-hydrogen (STH) efficiencies, accounting only for optical losses, are:

Single layer:	2.10%,	5.37%,	6.65%,	10.3%
Stacked layer:	6.55%,	9.22%,	10.2%,	12.9%

for $L = 200\,\mathrm{nm}$, $1\,\mu\mathrm{m}$, $2\,\mu\mathrm{m}$, and $20\,\mu\mathrm{m}$, respectively.

The STH efficiencies, accounting for $L_{\mathrm{D}} = 80$ nm with nonuniform carrier generation, are:

$$\begin{aligned} &\text{Single layer:} && 1.92\%,\ 1.87\% \\ &\text{Stacked layer:} && 5.97\%,\ 2.67\% \end{aligned}$$

for $L = 200\,\mathrm{nm}$ and $2\,\mu\mathrm{m}$, respectively.

The STH efficiencies, accounting for $L = 1\,\mu\mathrm{m}$ with nonuniform carrier generation, are:

$$\begin{aligned} &\text{Single layer:} && 2.39\%, 5.25\% \\ &\text{Stacked layer:} && 3.98\%,\ 9.00\% \end{aligned}$$

for $L_{\mathrm{D}} = 80\,\mathrm{nm}$ and $800\,\mathrm{nm}$, respectively.

V. KUBELKA–MUNK SPECTRUM OF $Gd_2Ti_2O_5S_2$

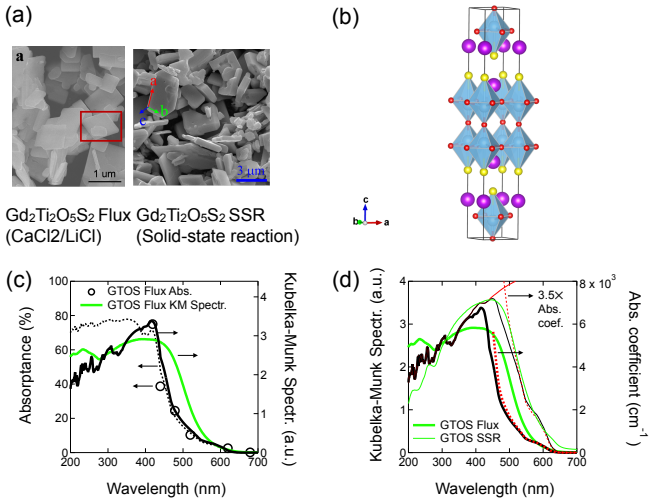

FIG. S1. (a) Scanning electron micrographs (SEM) of $Gd_2Ti_2O_5S_2$ prepared by flux growth (GTOS, flux) and by solid-state reaction (GTOS, ssr).[9] (SEM images taken from Ref. 10 and 9 for flux and ssr, respectively.) In this work, we focus primarily on GTOS (flux). (b) Conventional unit cell of $Gd_2Ti_2O_5S_2$; Gd (purple), Ti (blue), S (yellow), and O (red). In (c) and (d), open circles denote the measured absorptance, and the thick green line denotes the KM spectrum of GTOS (flux). (Data reproduced from Ref. 10.) (c) Thick black solid line: KM spectrum calculated by effective-medium theory [eqn (26) with R_∞ obtained from $R_{\rm em}$ in eqn (24)]; black dashed line: absorptance from the single-layer model [eqn (3)] with $L = 1$ μm. The measured absorptance follows both the calculated KM spectrum and the single-layer model. (d) KM spectra of GTOS (flux; thick green) and GTOS (ssr; thin green). (Data for ssr are reproduced from Ref. 9.) Black lines show effective-medium theory with $L = 1$ μm (thick) and $L = 2$ μm (thin). Red solid line: $(1-R)^2/(2R)$, with R calculated by DFT; the theoretical KM spectrum follows this relation at wavelengths shorter than the KM maximum. Red dashed lines: absorption coefficient α (thin dashed line is $3.5 \times \alpha$); the theoretical KM spectrum follows these near the band edge. Overall, agreement between experiment and theory is better for GTOS (ssr) than for GTOS (flux).

VI. INTERNAL QUANTUM EFFICIENCY WHEN THE LIGHT PENETRATION DEPTH IS SMALLER THAN THE PARTICLE SIZE

We solve the steady-state diffusion equation for the minority carrier density $p(r)$ using the radial coordinate r, incorporating both bulk recombination and photogeneration according to the Lambert–Beer law:

$$D\nabla^2 p(r) - kp(r) + g_0 \exp\left[-\alpha(a-r)\right] = 0, \tag{S43}$$

where $\nabla^2 = \partial^2/\partial r^2 + (2/r)\partial/\partial r$ is the Laplacian operator in spherical coordinates, and g_0 is the generation rate at the particle surface ($r = a, a = L/2$). We assume isotropic diffusion in a spherical particle of radius a, and impose the perfectly absorbing boundary condition $p(a) = 0$.

The radial current density $j(r)$ is defined as

$$j(r) = -4\pi r^2 D \frac{\partial p(r)}{\partial r}. \tag{S44}$$

The internal quantum efficiency I_{qe} is then defined as the ratio of extracted carriers to the total number of photogenerated carriers:

$$I_{qe} = \frac{j(a)}{\int_0^a dr\, 4\pi r^2 g_0 \exp\left[-\alpha(a-r)\right]}. \tag{S45}$$

An analytical expression for I_{qe} is obtained as

$$I_{qe} = \left\{ \alpha^3 a^2 L_\mathrm{D} \left[\left(1 + \frac{2\alpha L_\mathrm{D}^2}{a} - \alpha^2 L_\mathrm{D}^2 \right) \coth\left(\frac{a}{L_\mathrm{D}} \right) - \frac{L_\mathrm{D}}{a} - \alpha L_\mathrm{D} - \frac{\alpha^2 L_\mathrm{D}^3}{a} + \alpha^3 L_\mathrm{D}^3 \right.\right.$$
$$\left.\left. -2\frac{\alpha L_\mathrm{D}^2}{a} \exp(-\alpha a) \mathrm{csch}\left(\frac{a}{L_\mathrm{D}} \right) \right] \right\} \Big/ \left\{ \left(1 - \alpha^2 L_\mathrm{D}^2\right)^2 \left[2\left(1 - \alpha a - \exp(-\alpha a)\right) + \alpha^2 a^2 \right] \right\}. \tag{S46}$$

As expected, this expression reduces to $I_{qe} = 1$ in the limit $L_\mathrm{D} \to \infty$. We have numerically confirmed that $0 \le I_{qe} \le 1$ for representative values of L_D, α, and a.

In the limit $\alpha a < 1$ and $\alpha L_\mathrm{D} < 1$, eqn (S46) simplifies to

$$I_{qe} = 3\frac{L_\mathrm{D}}{a} \frac{(1+\alpha a)\coth(a/L_\mathrm{D}) - (L_\mathrm{D}/a)(1+2\alpha a) + \dfrac{2\alpha L_\mathrm{D}^2}{a} \tanh\left(\frac{a}{2L_\mathrm{D}}\right)}{1 + \frac{3}{4}\alpha a}. \tag{S47}$$

In the further limit $\alpha \to 0$, corresponding to uniform carrier generation, eqn (S47) reduces to the well-known result, eqn (33).[11]

VII. OPTICAL PROPERTIES OF $SrTiO_3$

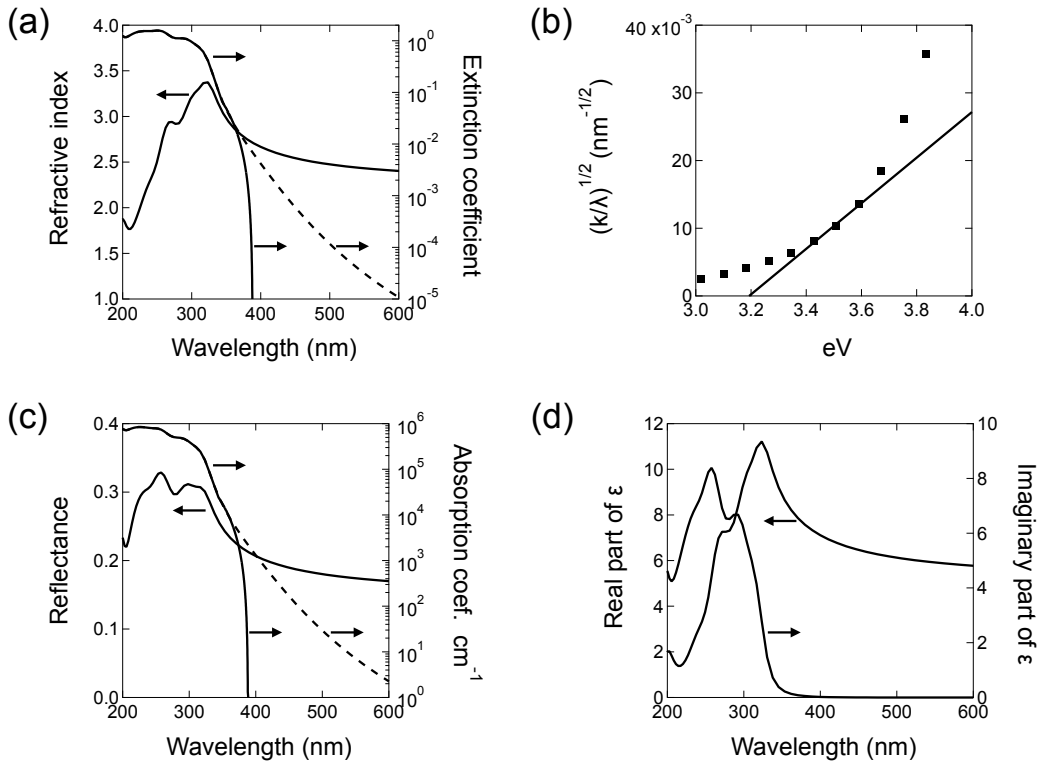

FIG. S2. Optical properties of $SrTiO_3$. In (a), the dashed curve shows the raw measured extinction coefficient k, which is orders of magnitude smaller than its peak yet remains positive above 388 nm (3.2 eV, the band gap). (Data of refractive index (n) and k are reproduced from Refs. 12 and 13.) The solid curve replaces the dashed data between 344 and 388 nm using the relation in (b). (a) Refractive index (n) and extinction coefficient (k) versus wavelength for a single crystal measured by spectroscopic ellipsometry.[12,13] (b) $\sqrt{k/\lambda}$ (with λ the wavelength). The straight line indicates the indirect–semiconductor relation used near the band edge (3.2 eV). (c) Reflectance and absorption coefficient computed from the n, k in (a): $\alpha = 4\pi k/\lambda$ and $R = \left[(n-1)^2 + k^2\right] / \left[(n+1)^2 + k^2\right]$. Curves derived from the raw (dashed) and modified (solid) k are compared. (d) Real ($\epsilon_{\rm r}$) and imaginary ($\epsilon_{\rm i}$) parts of the dielectric function, obtained from $\epsilon_{\rm r} = n^2 - k^2$ and $\epsilon_{\rm i} = 2nk$.

VIII. KUBELKA–MUNK SPECTRUM OF $SrTiO_3$

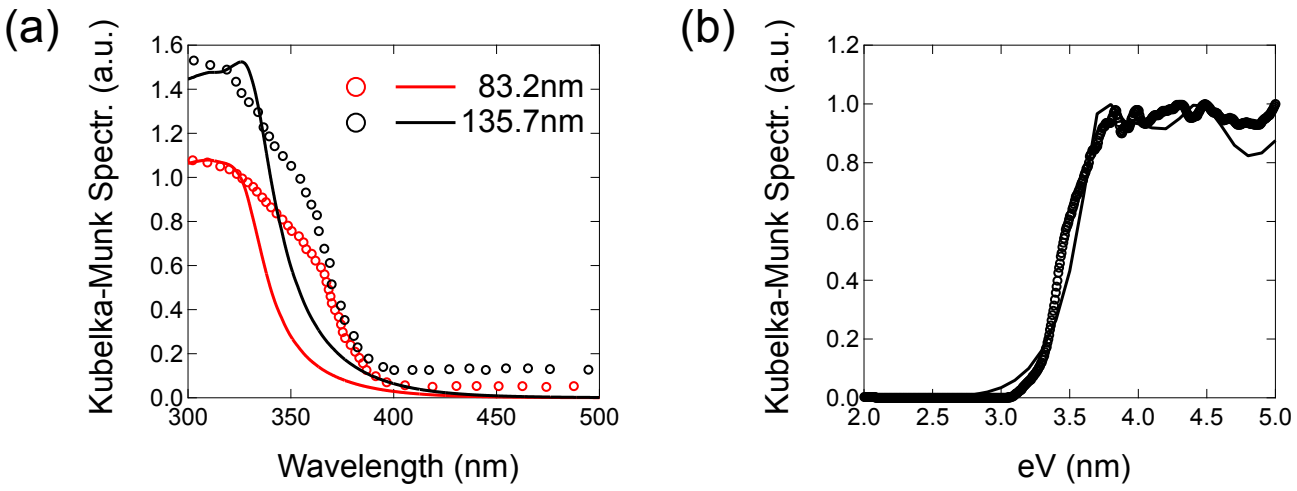

FIG. S3. Circles denote experimental Kubelka–Munk (KM) spectra of $SrTiO_3$. (Data for (a) and (b) are reproduced from Refs. 14 and 15, respectively.) Lines show effective-medium calculations using the extinction coefficient without modification (the dashed k in Fig. S2a). (a) KM spectra for mean particle sizes of 83.2 nm (black) and 135.7 nm (red).[14] (b) KM spectrum measured for dispersed particles with sizes between 100 nm and 1 mm.[15] The line is calculated assuming a representative particle size of 200 nm. The band-edge absorption observed in (a) may originate from defects and/or impurities.

IX. ABSORPTANCE AND KUBELKA–MUNK SPECTRUM OF $SrTiO_3$

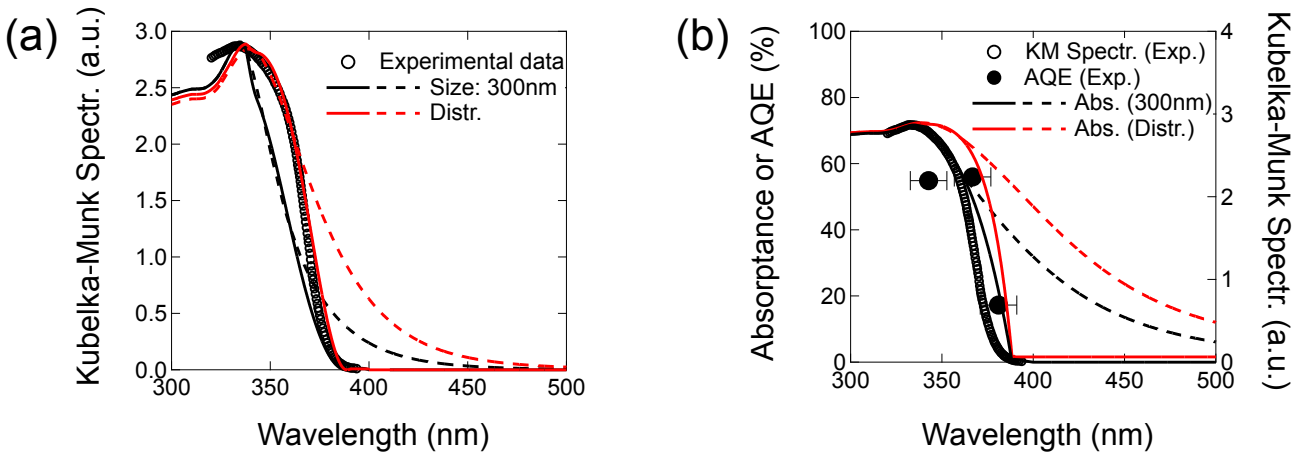

FIG. S4. Open and closed circles denote the experimental Kubelka–Munk (KM) spectrum and the absorptance of $SrTiO_3$:Al (Al content 0.96 mol%), respectively. (Data reproduced from Ref. 16.) Particle sizes are 200–500 nm.[16] Solid and dashed lines are effective-medium calculations using, respectively, an extinction coefficient modified to match the intrinsic band-gap absorption of $SrTiO_3$ and the unmodified extinction coefficient. Black lines correspond to a single particle size of 300 nm, while red lines use the particle-size distribution shown in Fig. 9 (d). (a) KM spectrum of $SrTiO_3$. (b) Absorptance and KM spectrum.

* k-seki@aist.go.jp

[1] L. D. Landau and E. M. Lifshits, *Electrodynamics of continuous media /*, 2nd ed., Course of theoretical physics / L.D. Landau & E.M. Lifshitz ; (Pergamon;, Oxford [Oxfordshire] ;, 1984(reprinted 2005).).

[2] G. Bader, P. V. Ashrit, F. E. Girouard, and V.-V. Truong, Appl. Opt. **34**, 1684 (1995).

[3] A. Vašíček, *Optics of Thin Films*, Series in physics (North-Holland Publishing Company, 1960).

[4] K. Forcht, A. Gombert, R. Joerger, and M. Köhl, Thin Solid Films **302**, 43 (1997).

[5] R. Joerger, K. Forcht, A. Gombert, M. Köhl, and W. Graf, Appl. Opt. **36**, 319 (1997).

[6] Wolfram Research, Inc., *Mathematica, Version 14.2.1* (Champaign, IL, 2025).

[7] ASTM International, "Reference air mass 1.5 spectra," `https://www.nrel.gov/grid/solar-resource/spectra-am1.5.html` (2003), aSTM G173-03.

[8] M. Kaneko, V. Nandal, K. Yamashita, and K. Seki, AIP Adv. **14**, 095115 (2024).

[9] R. Shoji, V. Nandal, K. Seki, X. Tao, A. Furube, T. Hisatomi, H. Yoshida, T. Takata, M. Kaneko, K. Yamashita, K. Domen, and H. Matsuzaki, EES Catal. **3**, 274 (2025).

[10] H. Yoshida, Z. Pan, R. Shoji, V. Nandal, H. Matsuzaki, K. Seki, L. Lin, M. Kaneko, T. Fukui, K. Yamashita, T. Takata, T. Hisatomi, and K. Domen, Angew. Chem. Int. Ed. **62**, e202312938 (2023).

[11] V. Nandal, R. Shoji, H. Matsuzaki, A. Furube, L. Lin, T. Hisatomi, M. Kaneko, K. Yamashita, K. Domen, and K. Seki, Nat. Commun. **12**, 7055 (2021).

[12] V. Trepakov, A. Dejneka, P. Markovin, A. Lynnyk, and L. Jastrabik, New J. Phys. **11**, 083024 (2009).

[13] M. N. Polyanskiy, Sci. Data **11**, 94 (2024).

[14] S. Wang, H. Gao, X. Yu, S. Tang, Y. Wang, L. Fang, X. Zhao, J. Li, L. Yang, and W. Dang, J. Mater. Sci.: Mater. Electron. **31**, 17736 (2020).

[15] T. K. Townsend, N. D. Browning, and F. E. Osterloh, Energy Environ. Sci. **5**, 9543 (2012).

[16] Y. Goto, T. Hisatomi, Q. Wang, T. Higashi, K. Ishikiriyama, T. Maeda, Y. Sakata, S. Okunaka,

H. Tokudome, M. Katayama, S. Akiyama, H. Nishiyama, Y. Inoue, T. Takewaki, T. Setoyama, T. Minegishi, T. Takata, T. Yamada, and K. Domen, Joule **2**, 509 (2018).